2016

A multi-sensor system for high throughput field phenotyping in soybean and wheat breeding

Geng Bai
University of Nebraska - Lincoln, gbai2@unl.edu

Yufeng Ge
University of Nebraska - Lincoln, yge2@unl.edu

Waseem Hussain
University of Nebraska - Lincoln, waseem.hussain@unl.edu

P. Stephen Baenziger
University of Nebraska - Lincoln, pbaenziger1@unl.edu

George L. Graef
University of Nebraska - Lincoln, ggraef1@unl.edu

Computers and Electronics in Agriculture 128 (2016) 181–192

Contents lists available at ScienceDirect

Computers and Electronics in Agriculture

journal homepage: www.elsevier.com/locate/compag

Original papers

A multi-sensor system for high throughput field phenotyping in soybean and wheat breeding

Geng Bai [a], Yufeng Ge [a,*], Waseem Hussain [b], P. Stephen Baenziger [b], George Graef [b]

[a] Department of Biological Systems Engineering, University of Nebraska-Lincoln, Lincoln, NE 68583, USA
[b] Department of Agronomy and Horticulture, University of Nebraska-Lincoln, Lincoln, NE 68583, USA

ARTICLE INFO

Article history:
Received 10 May 2016
Received in revised form 22 August 2016
Accepted 28 August 2016
Available online 14 September 2016

Keywords:
High throughput field phenotyping
Canopy reflectance
Canopy temperature
LabVIEW
RGB image

ABSTRACT

Collecting plant phenotypic data with sufficient resolution (in both space and time) and accuracy represents a long standing challenge in plant science research, and has been a major limiting factor for the effective use of genomic data for crop improvement. This is particularly true in plant breeding where collecting large-scale field-based plant phenotypes can be very labor intensive and costly. In this paper we reported a multi-sensor system for high throughput phenotyping in plant breeding. The system comprised five sensor modules (ultrasonic distance sensors, thermal infrared radiometers, NDVI sensors, portable spectrometers, and RGB web cameras) to measure crop canopy traits from field plots. A GPS was used to geo-reference the sensor measurements. Two environmental sensors (a solar radiation sensor and air temperature/relative humidity sensor) were also integrated into the system to collect simultaneous environmental data. A LabVIEW program was developed to control and synchronize measurements from all sensor modules and stored sensor readings in the host computer. Canopy reflectance spectra (by portable spectrometers) were post processed to extract NDVI and red-edge NDVI spectral indices; and RGB images were post processed to extract canopy green pixel fraction (as a proxy for biomass). The sensor system was tested in a soybean and wheat field trial. The results showed strong correlations among the sensor-based plant traits at both early and late growing season. Significant correlations were also found between the sensor-based traits and final grain yield at the early season (Pearson's correlation coefficient r ranged from 0.41 to 0.55) and late season (r from 0.55 to 0.70), suggesting the potential use of the sensor system to assist in phenotypic selection for plant breeding. The sensor system performed satisfactorily and robustly in the field tests. It was concluded that the sensor system could be a powerful tool for plant breeders to collect field-based, high throughput plant phenotyping data.

1. Introduction

Next generation sequencing technologies enable scientists to conduct plant genotyping with ever increasing speed and declining cost (Shendure and Ji, 2008). The use of genomic data, however, must be coupled with high quality phenotypic data to meet its full potential. The challenge lies in the fact that characterizing plant phenotypes is costly and time consuming, which represents a major bottleneck in linking genotypes to phenotypes (Furbank and Tester, 2011). Many believe that, if this challenge can be mastered, we will be able to spark a new green revolution to greatly enhance the productivity of all major food, feed, and energy crops around the world. This success would be an essential part of the solutions to solve the global food security problem by 2050 when a world population of 9.7 billion is projected (Ray et al., 2012). Due to its perceived importance, intensive research efforts are currently underway on automated high throughput plant phenotyping (Furbank and Tester, 2011).

Much of the research on high throughput phenotyping has focused on the measurement of single plants using automated imaging in environmentally controlled greenhouses (Campbell et al., 2015; Fahlgren et al., 2015). These greenhouse based systems are proven useful to quantify certain plant traits such as biomass or growth rate, but they also face a number of major limitations. First, the limited space of imaging chambers makes it difficult to measure large plants when they pass certain stages of vegetative growth. Second, plants in greenhouses are grown in artificial environments (such as pot, soil, water and nutrient distribution, closed aerial environment, and artificial lighting) that can significantly alter the normal pattern of plant growth and development

* Corresponding author at: Department of Biological Systems Engineering, 209 Chase Hall, East Campus, University of Nebraska-Lincoln, Lincoln, NE 68583, USA.
E-mail address: yge2@unl.edu (Y. Ge).

http://dx.doi.org/10.1016/j.compag.2016.08.021
0168-1699/

(White et al., 2012). In addition, plants are grown in densely populated plots in the field, which affects the kinds of traits that can be measured effectively at the plot level compared to those at the single plant level. For example, side-view images are common in greenhouse phenotyping to measure plant height. In the field, however, plot height is usually measured above crop canopy with a height sensor. In summary, plant phenotyping in the greenhouse may be of limited relevancy and not directly translatable to field research (White et al., 2012; Nelissen et al., 2014).

Many authors have advocated field-based phenotyping systems and approaches for plant breeding (Passioura, 2012; White et al., 2012; Araus and Cairns, 2013). However, the development of field-based phenotyping systems has been slower than their greenhouse counterparts. There have been numerous reports in the literature on the vehicle based sensor systems for crop measurements in the fields; and most of them were developed in the context of precision agriculture (Scotford and Miller, 2004; Noh et al., 2006; Sui and Thomasson, 2006; Sui et al., 2008; Farooque et al., 2013; Wang et al., 2014).

Montes et al. (2011) reported a field phenotyping system employing a light curtain and spectral reflectance sensors for the biomass determination of maize in early developmental stages. To measure the canopy water mass of tropical maize hybrids, Winterhalter et al. (2011) developed a sensor system comprising a spectroradiometer and infrared thermometer. Romano et al. (2011) used a thermal imaging system to distinguish tropical maize genotypes in water stress. Comar et al. (2012) reported a semi-automatic sensing system for phenotyping wheat cultivars in field conditions. The system was based on a hyperspectral radiometer and two RGB cameras, which allowed the authors to calculate two vegetation indices (correlated to leaf chlorophyll) and the fraction of green area per unit ground area. Andrade-Sanchez et al. (2014) developed a field phenotyping system that incorporated three sensing modules to measure plant canopy height, temperature, and NDVI (Normalized Difference Vegetation Index). Three separate data loggers were used to record the sensor data, which were post processed and merged to individual plots for further analysis. Sharma and Ritchie (2015) reported a high throughput phenotyping system for cotton. This system included sensors that automatically measured plant height, ground cover fraction, NDVI, and canopy temperature.

For the sensor systems being suitable for high throughput field phenotyping, they should meet two requirements. First, the system should measure multiple plots simultaneously to improve throughput. Second, the system should be able to measure and fuse a multitude of traits that take different data formats (point measurements, spectra (1-d arrays), and images (2-d arrays)). There are many off-the-shelf sensors that are suitable for plant measurement, but challenge remains to bring them into an integrated system to maximize the capability and efficiency of phenotyping (in terms of sensor type and number, and data formats).

In this paper, we reported the development of a multi-sensor system aiming at collecting high throughput, plot-level trait measurements for plant breeding. Emphases were given to the integration of various sensing modules enabling the collection of collocated and georeferenced data including point measurements, reflectance spectra, and optical images, which facilitated subsequent data post processing and trait analysis. We also reported the field testing of the system in soybean and wheat field trials.

2. Materials and methods

2.1. High throughput field phenotyping multi-sensor system

2.1.1. The platform

The platform that carried the sensor system (Fig. 1) was based on the proximal sensing cart in White and Conley (2013). There had been a number of platforms proposed for field phenotyping including manually operated carts, self-propelled tractors, unmanned aerial vehicles (UAVs), and remote sensing towers (Ahamed et al., 2012; Deery et al., 2014; Sankaran et al., 2015). Our focus was mainly on breeding trials which were no more than a few acres in size. We therefore chose a manually operated platform that was adequate to cover the area within a few hours. Compared to self-propelled tractors, this platform caused minimum mechanical disturbance to plants and soil compaction to the fields. Compared to UAVs, it was not limited by payload and can carry more sensors for simultaneous measurements of different traits.

2.1.2. Sensing modules employed on the sensor system

The sensing modules employed on the field phenotyping system are given in Table 1. The important sensor parameters and the plant traits targeted by these sensors are also summarized in Table 1. Fig. 2 shows one sensor suite to measure one crop row (or plot), and the system can accommodate up to four sensor suites.

The ultrasonic sensor outputs analog voltage signals (0–10 V) proportional to the distance D between the sensor and plant canopy. The linear relationship between the voltage output and D was found by a sensor-specific calibration procedure conducted in the lab before field surveys. The canopy height (h) was calculated by the sensor height (H, which was the distance between the sensor and the ground and was precisely measured with a tape mea-

Fig. 1. The platform to mount the multi-sensor system for high throughput field phenotyping.

Table 1
Sensing modules, their parameters for system integration, and the canopy trait measured by each sensor.

Sensor	Sensor Model and Manufacturer	Powered by	Output	Field of view	Canopy trait measured
Ultrasonic sensor	ToughSonic30, Senix Corporation, Hinesburg, Vermont	12 VDC	Analog Voltage	NA	Height
NDVI sensor	SRS, Decagon Devices, Pullman, Washington	12 VDC	Digital (SDI-12)	18°	NDVI
Thermal infrared radiometer	SI-131, Apogee Instruments, Inc., Logan, Utah	2.5 VDC	Analog Voltage	14°	Temperature
Portable spectrometer	CCS175, Thorlabs Inc., Newton, New Jersey	5 VDC (via USB)	Digital (via USB)	13°	Reflectance spectra
RGB camera	C615, Logitech	5 VDC (via USB)	Digital (via USB)	33° by 20°	RGB image

NDVI = Normalized Difference Vegetation Index.
SDI-12 (www.sdi-12.org) was converted to RS232 using a RS232 to SDI12 converter (H-4191, YSI Incorporated, Yellow Springs, Ohio) before connected to the data acquisition board.
Field of view was defined by the half-angle of the conic shape subtended by the unobstructed view of the sensor.

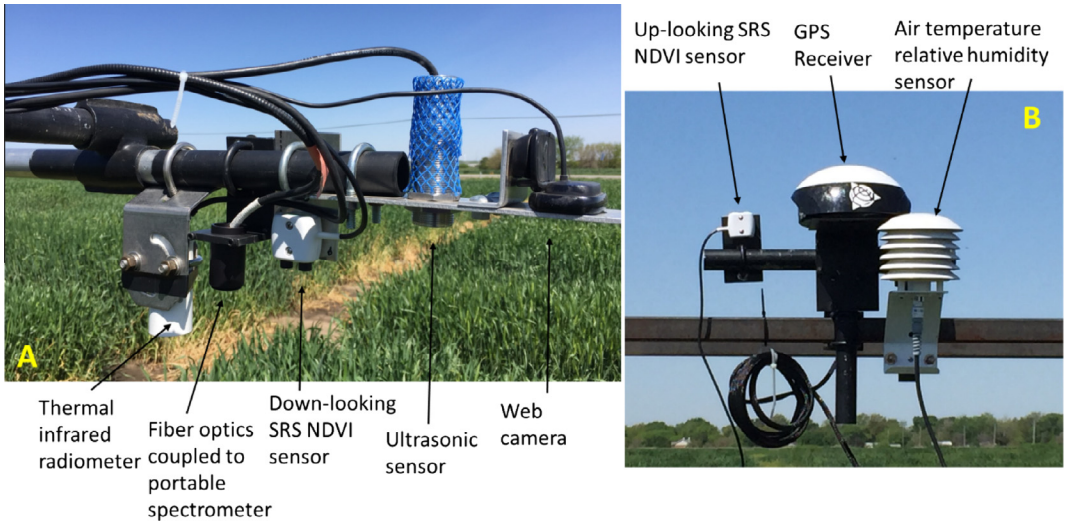

Fig. 2. The five sensing modules mounted on a sensor bar to measure one crop row or plot (A); and the GPS receiver, air temperature/relative humidity sensor, and up-looking SRS NDVI sensor mounted at the center of the platform (B).

sure before each field survey) less the distance (i.e., $h = H - D$). The sensor had a specified repeatability of 0.2% of active readings.

The NDVI sensors were passive-type and rely on solar radiation to function. They are different from active-type Green Seeker or Crop Circle NDVI sensors which use their own frequency-modulated LED light sources for illumination and crop canopy reflectance retrieval. The sensor had an up-looking unit (pointing to the sky, Fig. 2) to measure the down-welling solar radiation at the NIR (near infrared) and red band (NIR_D and RED_D), and a down-looking unit (pointing to plant canopy) to measure the up-welling reflected solar radiation (NIR_U and RED_U). Canopy NDVI was then calculated by using the equation below.

$$NDVI = (\rho_{NIR} - \rho_{RED})/(\rho_{NIR} + \rho_{RED}) = \left(\frac{NIR_U}{NIR_D} - \frac{RED_U}{RED_D}\right) \Big/ \left(\frac{NIR_U}{NIR_D} + \frac{RED_U}{RED_D}\right) \quad (1)$$

The sensor system can accommodate up to four down-looking NDVI units (one for each plot under measurement), but required only one up-looking unit (mounted at the center of the platform, Figs. 1 and 2) to compensate for the fluctuation of solar radiation for NDVI measurement.

The thermal infrared radiometer (TIR, spectral response bandwidth 8–14 μm) sensor output differential voltage signals (sensitivity 20 μV/°C) proportional to the temperature difference between the target surface (i.e., plant canopy) and the body temperature of the TIR detector (which was measured by an onboard thermistor). The calibration equations provided by the manufacturer were then used to convert the differential voltage signals to canopy temperature (The sensor specific calibration gave an overall measurement accuracy of ±0.2 °C).

Each portable spectrometer was coupled with a fiber optics cable (4-m long, 200-μm core diameter, 0.22 numeric aperture, and pointing to plant canopy) to measure canopy reflectance. The spectrometers had a spectral range from 500 to 900 nm, and with a narrow spectral sampling interval of 1/6 nm (six data points per nm). This spectral range and sampling interval allowed the retrieval of many useful vegetation indices such as NDVI, Photochemical Reflectance Index (PRI $= \frac{\rho_{531} - \rho_{570}}{\rho_{531} + \rho_{570}}$, Garbulsky et al., 2011), and Solar Induced Fluorescence (SIF, Meroni et al., 2009; Guanter et al., 2013). The sensitivity of the photo detector employed by the spectrometer is 160 V/(lx·s) with a signal to noise ratio of 2000:1. Similar to the NDVI sensors, portable spectrometers were also passive-type, meaning one spectrometer coupled with an up-looking fiber optics cable (with a cosine corrector) was used to provide the baseline hemispherical down-welling spectrum of solar radiation (Fig. 2). Canopy reflectance was calculated by taking the ratio between the up-welling spectra and the down-welling spectra.

Finally, Logitech web cameras were employed to capture RGB images from individual plots. Images were taken roughly 1.0 m above the canopy. The web cameras had a resolution of 1920 × 1080 pixels, and were controlled through USB connection for image acquisition without a frame grabber. This significantly simplified the complexity of system hardware and was the main reason to use the USB web cameras.

In addition to the above sensing modules for plant trait measurement, we also integrated two environmental sensors into the system: a solar radiation sensor (model LI-200, LICOR Biosciences,

Lincoln, Nebraska) and an air temperature and relative humidity sensor (model CS215-L, Campbell Scientific Inc., Logan, Utah). We used these co-registered environmental sensor readings to account for the influence of environmental fluctuation on crop trait measurements. For example, canopy temperature T_c minus air temperature T_a was a better probe for canopy thermal status than T_c alone, especially when air temperature fluctuated substantially during the field survey.

A high quality GPS (AgGPS 216, Trimble Navigation Ltd., Sunnyvale, California) was used to geo-reference sensor readings. The GPS used WAAS correction and had a pass-to-pass positioning accuracy of 20 cm. This was considered adequate for our applications when compared to a 0.75 m row width of soybean and 1.5 m plot width of wheat.

The distance between the sensor bar (Fig. 1) and crop canopy was important for the collection of high quality plant phenotypic data. In our study we adjusted the height of the sensor bar during the growing season such that it was placed approximately 1.0 m above the canopy (Supplemental Fig. 1). This distance was determined by examining the field of view of each sensor to ensure a representative subarea in each plot was scanned (Supplemental Fig. 1). As mentioned earlier, the exact height of the sensor bar above soil was measured at the beginning of each field survey.

2.1.3. Hardware integration and software of the system

A laptop computer was used as a controlling unit to control and synchronize measurements from all sensor modules. A USB data acquisition board (Model U6, LABJACK, Lakewood, Colorado) was used to read measurements (voltage signals) from the ultrasonic sensors, TIR sensors, and the solar radiation sensor through its analog input ports. NDVI sensors and air temperature/relative humidity sensors were also read by LABJACK U6 through its serial ports (RS232). Measurements from portable spectrometers (in the form of spectra, ~2400 data points per spectrum) and web cameras (1920 × 1080 pixels per image) were captured directly with the USB ports on the computer (through a USB hub due to the number of USB ports needed in total).

A LabVIEW program (Version 2014, National Instruments, Austin, Texas) was developed to run on the laptop computer for the acquisition of sensor measurements. The main functions of the program were as follows.

(1) Read the sensor outputs (Ultrasonic sensors, TIR sensors, and the solar radiation sensor) from analog input ports of the LABJACK U6 board and apply their respective calibration equations to convert sensor voltages to physical quantities (cm, °C, and W/m^2).
(2) Read the up-looking and down-looking NDVI sensor units via RS232 and apply Eq. (1) to convert the readings to NDVI; and read the air temperature/relative humidity sensor also via RS232.
(3) Read the spectral measurements of plot canopy from both up-looking and down-looking portable spectrometers.
(4) Trigger the web cameras and capture RGB images of plot canopy through LabVIEW's IMAQdx vision acquisition module.
(5) Record the NMEA-0183 messages (GPRMC sentence) from the GPS receiver, extract longitude and latitude coordinates, and convert them into UTM NAD83 projected coordinate system. Depending on the number of sensor suites used and platform travel direction, position correction was implemented to tag the corrected GPS coordinates to each plot reading.
(6) Store the sensor readings on the computer. Point measurements including GPS, height, canopy temperature, NDVI, air temperature, relative humidity were stored in a spreadsheet (CSV format) file. Reflectance spectra and plot images were stored as individual files using a predetermined file naming pattern so that they can be associated with the individual records in the CSV file in post processing.

The front panel of the LabVIEW program (Fig. 3) displayed the readings from all sensor modules in real time, including reflectance spectra and RGB images. This allowed us to quickly know when a

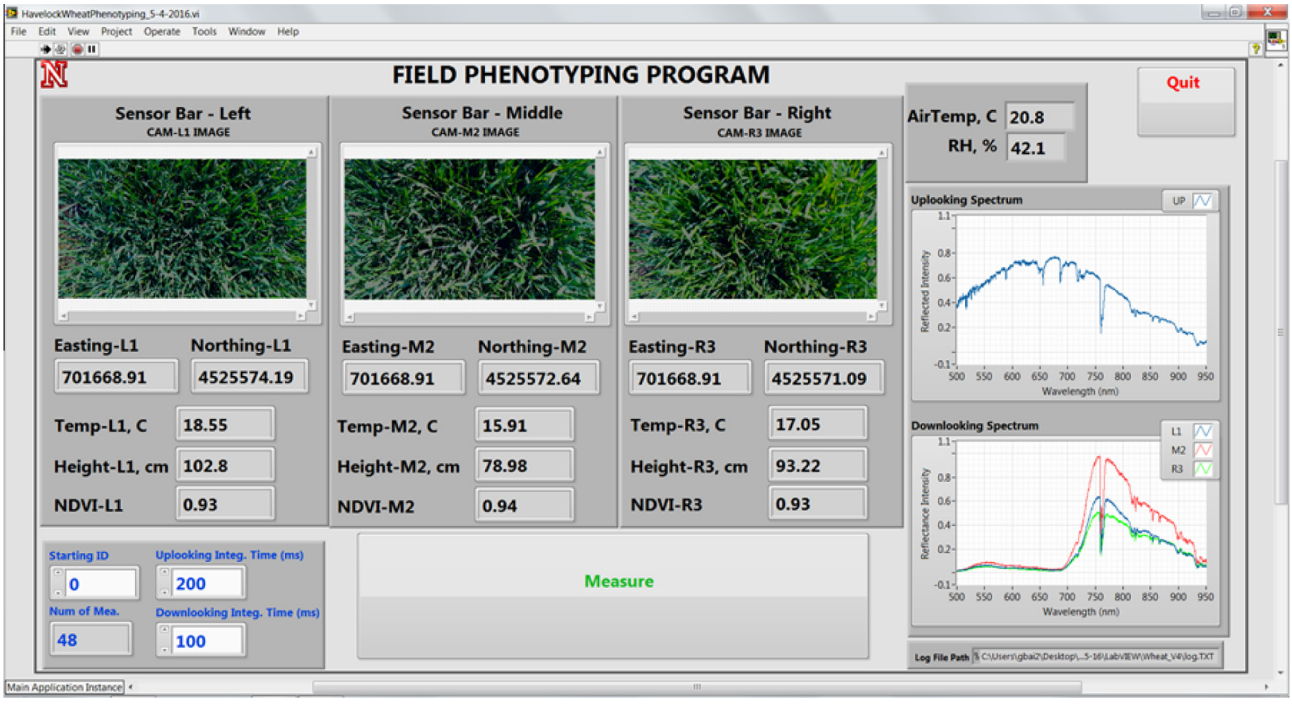

Fig. 3. The front panel of the LabVIEW program of the field phenotyping sensor system.

problem occurred (such as the malfunction of certain sensors) during field data collection. LabVIEW subVIs for some selected program functions are provided in Supplemental Fig. 2.

We employed a "stop-measure-go" fashion to take the plot-level phenotypic measurements with the sensor system. That is, the operators manually pushed the platform to the center of the plots and pressed the "measure" button on the front panel of the program (Fig. 3) to record the measurements. This was different from some other field phenotyping studies in which "continuous measurement" was employed (Andrade-Sanchez et al., 2014). The main reason was that some sensor modules in our system had slow response time. For example, the TIR sensors had a response time of 0.6 s. The portable spectrometers also required integration time of 150 ms under normal sunny sky conditions to achieve strong signal level. Since the system controlled four groups of sensors, these slow response sensors made it not practical for a continuous data logging mode at a rate of, for example, 1 Hz. The disadvantage of the "stop-measure-go" mode was that the throughput of measurement inevitably decreased. There were also two advantages. Firstly, the plot images were all captured without blurry. Secondly, all sensor measurements were aligned with plots, which eliminated the need of post processing to remove measurements on plot borders and alleys.

2.2. Testing of the multi-sensor system for field phenotyping

The multi-sensor system was tested in a soybean and wheat field trial on the University of Nebraska-Lincoln's research farms in 2015.

The soybean experiment was a water use experiment consisting of 15 soybean genotypes and two water treatments (well-watered versus drought). The treatments were replicated four times giving a total of 120 plots. The well-watered plots were irrigated with surface drip irrigation whereas the drought plots were covered with plastic films on soil surface to prevent rain infiltration. Each plot had four rows of soybean, and was six m long and three m wide. Soybean was plant on May/22 and harvested on Sep/30. Field data collection with the sensor system was conducted six times during the growing season.

The wheat experiment was a quantitative trait loci (QTL) mapping study which involved 204 recombinant inbred lines (RILs) plus three checks. An augmented design with 12 blocks was used to evaluate all wheat lines, each block containing 17 unique RILs (un-replicated) plus the three checks (replicated for each block). This gave a total of 240 plots. Each plot was approximately 4.5 m long by 1.6 m wide and had four rows of wheat. Wheat was planted on Sep/29/2014 and harvested on Jul/20/2015. Field data collection was conducted seven times during the season. See Supplemental Fig. 3 for the field maps of the soybean and wheat plots.

At the end of the season, soybean and wheat grain yield data were collected from each plot, and were used to correlate with the in-season crop traits measured by the sensor system.

2.3. Sensor data post processing and analysis

Plot canopy height, NDVI by the NDVI sensor (referred to as NDVI-SRS), canopy temperature, solar radiation, and air temperature and relative humidity were point measurements, and used directly without further processing.

For canopy reflectance spectra measured by the portable spectrometers, we first took the ratio between the down-looking spectra and the up-looking spectra to obtain canopy reflectance spectra. Second, we derived from the reflectance spectra two spectral indices, namely NDVI and red-edge NDVI, for further analysis [referred to as NDVI-spec (to distinguish from NDVI-SRS) and RE-NDVI-spec]. NDVI-spec was calculated from reflectance at 630 and 800 nm. RE-NDVI-spec was calculated from reflectance at 705 and 750 nm. Compared to NDVI, red-edge NDVI is more sensitive to green vegetation and leaf area toward the late growing season (Sims and Gamon, 2002).

Canopy RGB images were used to extract green pixels and calculate green pixel fraction (GPF). It is a useful and sensitive index to estimate vegetation biomass, in particular in early season before canopy closure. Illumination variations (day-to-day variation and within-day variation) and shadows (casted by clouds and the sensor platform itself) made the development of automatic image segmentation quite challenging. We tried a couple of different methods and found that converting the images from RGB to L∗a∗b color space and then using *a* component for thresholding (using Otsu's adaptive thresholding algorithm) gave the most robust result to segment green pixels from the background across various solar illumination levels and shadows. After image segmentation, total green pixel count was divided by image size to obtain GPF.

After the analysis, there were six sensor-based traits measured by the field phenotyping sensor system. They were: Height, Tc-Ta (canopy temperature minus air temperature), NDVI-SRS (NDVI measured by the NDVI sensor), NDVI-spec (again, NDVI measured by the portable spectrometers), RE-NDVI-spec (red-edge NDVI measured by the portable spectrometers), and GPF (Green Pixel Fraction from RGB images). We then examined (1) the inter-correlation among these six sensor-based traits, (2) the temporal dynamics of these traits across the growing season, and (3) the correlation between these six sensor-based traits and final grain yield.

3. Result and discussion

3.1. Overall performance of the multi-sensor system in the fields

The sensor system was tested to conduct field survey six times for soybean and seven times for wheat during the growing season. Each field survey lasted for two to three hours and was carried out between 10 AM and 3 PM (which was the most appropriate time window for field phenotyping data collection). With the highest survey speed, we covered all 240 wheat plots in 1.0 h, including the time spent on end-row turning. This was equivalent to a survey speed of 0.2 ha (or 0.5 acre) per hour. This speed was lower than the speed of 0.84 ha per hour reported in Andrade-Sanchez et al. (2014). This was mainly because our platform was manually operated with lower travelling speeds through the plots. More sensors with slower response time also contributed to this lower survey speed. The speed could be improved if the system was mounted on a self-propelled vehicle. On the other hand, many breeding programs use land of one or two acres. Therefore, even with this low survey speed, a breeding field can be adequately covered in a few hours.

The platform can be easily maneuvered by two operators, with little problem to navigate through the plots or turn at the end rows. The mechanical disturbance to the plots was not discernable. The mechanical structure of the phenotyping platform was stable and durable. No mechanical or structural failure occurred during the season long field surveys. It is important to note that both the wheat and soybean fields were flat with a slope of 0–2%. Field slope would have large impact on the survey speed and mechanical stability of our platform. Therefore, more extensive testing under various field conditions is needed. During the first two surveys in the wheat field, there was a GPS logging error in the LabVIEW program and it was fixed thereafter. No other software warnings or exceptions occurred in the subsequent field surveys. All sensor modules functioned properly. Overall the field phenotyping system performed satisfactorily and robustly in the field test. In the following sections, we present the field data collected by the sensor system

with an emphasis on soybean. There were a few reports on wheat field phenotyping (Comar et al., 2012; Kipp et al., 2014) but the information on soybean was not previously reported, to the best of our knowledge.

3.2. Plot level canopy reflectance spectra and RGB images

Fig. 4(A) and (B) shows the average reflectance spectra of the wheat plots (May/13) by the up-looking and down-looking portable spectrometers. Due to high spectral resolution, several fine absorption features of solar radiation can be identified. The spectral window in the up-looking graph indicates the large variation of solar intensity during the field survey; whereas the spectral window in the down-looking graph indicates the variation of reflected solar intensity from the wheat plots. The Fraunhofer O_2-A (at 760 nm) and O_2-B (at 687 nm) lines are visible in both graphs. These two spectral absorption bands coincide with the two chlorophyll fluorescence peaks, which can be utilized to detect SIF of plants in a strong reflectance background. SIF is a useful index to probe plant stress as it directly measures chlorophyll and photosynthetic activity.

Fig. 5 shows the average canopy reflectance spectra of the soybean plots derived from ratioing the spectra from the down-looking and up-looking spectrometers. Ratioing successfully removed the absorption features in the solar spectrum. The reflectance spectrum at early season exhibited a relative low contrast between the visible (500–700 nm) and the NIR region (750–900 nm). This was due to the fact that soil spectrum was mixed with the vegetation spectra when canopy was open (soil had a much flatter transition from visible to NIR). As the season progressed and plant canopy continued to close, reflectance values in the visible region continued to decrease (caused by higher chlorophyll absorption) whereas reflectance values in the NIR range continued to increase (caused by stronger structural reflection of thicker plant canopy), which is consistent with our knowledge of canopy reflectance. At late season (Sep/2), the average plot reflectance began to show some characteristic of crop maturity (wilted plant leaves in canopy), with high reflectance in visible and low reflectance in NIR.

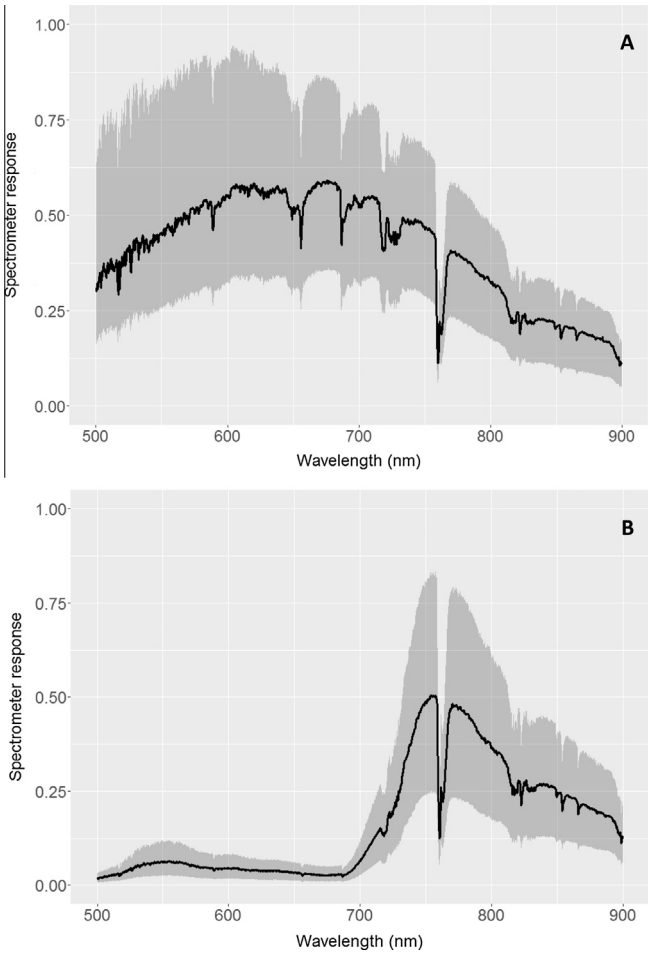

Fig. 4. The spectral intensity curves captured by the up-looking portable spectrometer (A: relative energy intensity of down-welling solar radiation) and the down-looking portable spectrometers (B: relative energy intensity of reflected solar radiation from crop canopy). The black lines are the mean spectra of all plots and the gray windows are the maximum and minimum bounding boxes showing the variation.

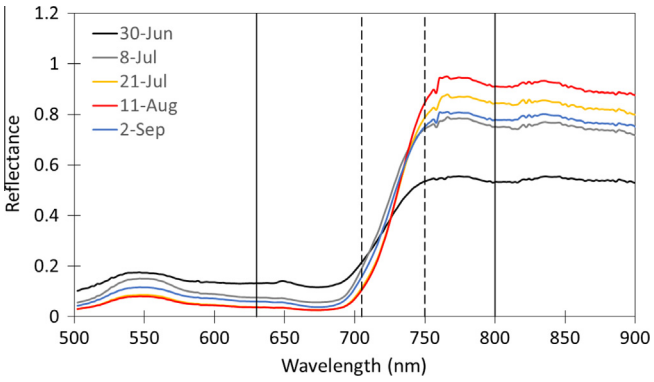

Fig. 5. The average canopy reflectance spectra of the soybean plots derived from the up-looking and down-looking portable spectrometers on different dates during the season. The solid vertical lines denote the wavelengths to calculate NDVI (630 and 800 nm) and the dashed vertical lines denote the wavelengths to calculate red-edge NDVI (705 and 750 nm).

Because different plant chemical constituents (such as pigments and water) and physiological processes can influence optical properties of leaf or canopy, many vegetation indices are developed as rapid and non-destructive probes to measure plant stress. Among them, NDVI is most widely used to sense vegetation abundance and nitrogen status. But other spectral indices can also be very useful for plant phenotyping. In addition to SIF discussed earlier, photochemical reflectance index (PRI) is another spectral index to surrogate light use efficiency and xanthophyll cycle of plants (Gamon et al., 1997; Garbulsky et al., 2011). Unlike NDVI, PRI and SIF require reflectance measured at fine spectral resolution. This makes the construction of dedicated optical sensors for these spectral indices challenging; and high resolution spectrometers therefore would be essential sensors to extract these useful spectral indices for plant phenotyping.

Fig. 6 gives an example of RGB images collected from a soybean plot on the six field survey days during the season. The color tone of these images was quite different, due to the day to day variation in solar radiation (i.e., sunny versus overshadow days). While not shown in this figure, the influence of short-term fluctuation of solar illumination (within the field survey window) can also be substantial. At early stage, canopy was open and there was good contrast between plants and soil, and image processing was relatively simple. Green pixel segmentation became more difficult as the season progressed. The canopy structure made part of the canopy sunlit and other parts shaded. Shades were also from the sensor platform itself. On 9/2 as soybean progressed into maturation, a portion of plant canopy turned yellow. These factors are challenges to develop a robust image processing algorithm for GPF estimation.

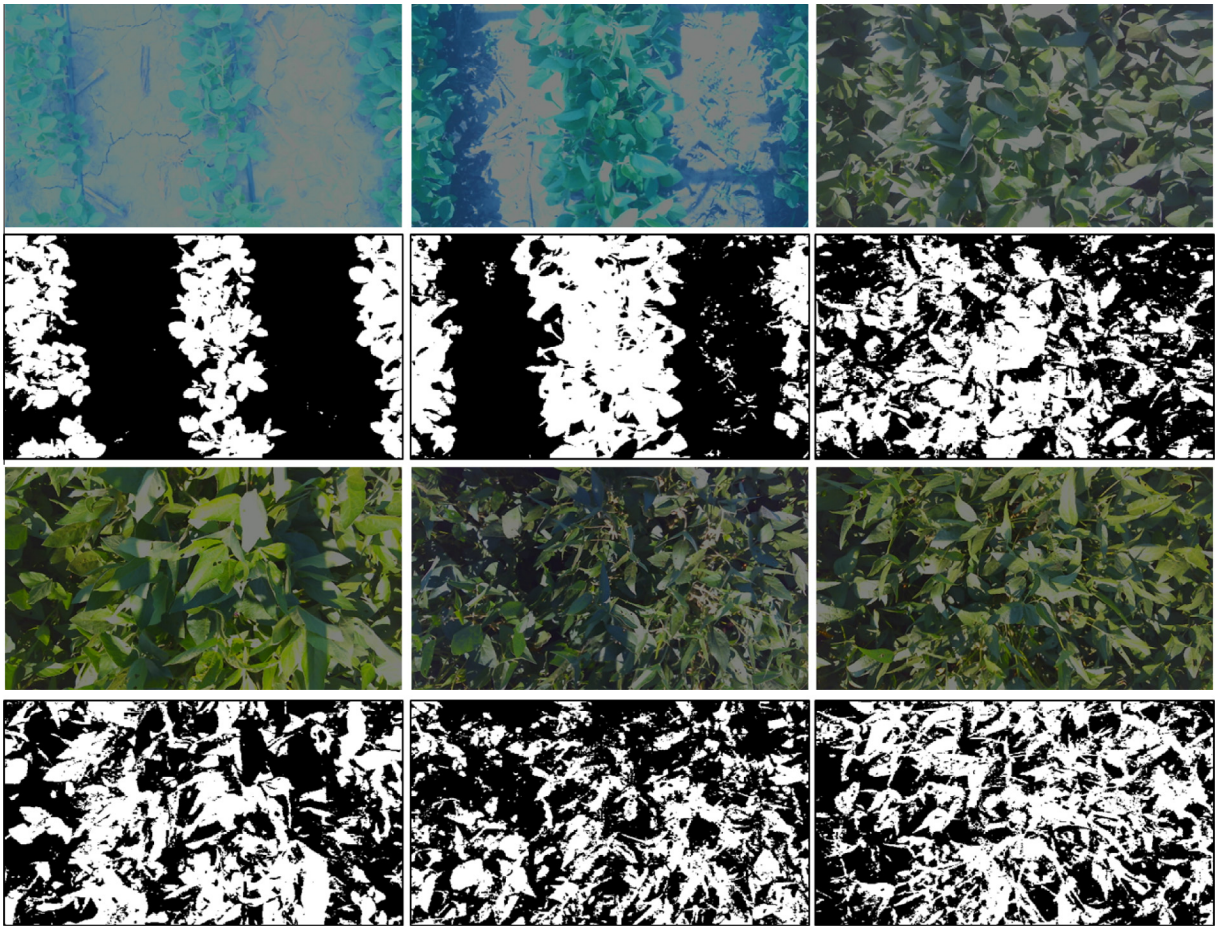

Fig. 6. RGB images collected by the sensor system from a soybean plot at the six dates during the season. Black and white images below the raw images are the results of image segmentation to calculate green pixel fraction.

3.3. Inter-correlations among sensor-based trait measurements

Figs. 7–9 show the inter-correlation among the six sensor-based soybean traits on Jun/30, Jul/31, and Sep/2, respectively. In Fig. 7, strong and significant correlations existed among all the variables. The highest correlations were among the three vegetation indices. This is not surprising because they all measure the same biophysical parameter. The consistency among NDVI-SRS, NDVI-spec, and RE-NDVI-spec provides an internal validation that both SRS sensors and portable spectrometers were working properly in the field. Tc-Ta shows consistent (and significant) negative correlations with all other variables. The amount of plant biomass in each plot appears to play a dominant role for the correlation pattern on this early season day (when the canopy wasn't closed yet and soil fraction was still high when viewed from above). Height, NDVIs, and GPF all measured certain aspect of biomass. Vegetation usually shows lower surface temperature than air temperature (due to active transpiration) whereas the surface temperature of soil is usually higher than that of air temperature during middays (when field data collection was conducted). Therefore, a lower Tc-Ta indicates the vegetation fraction is higher in TIR sensor's field of view, which explains the strong negative correlation between Tc-Ta and all other five parameters.

On Jul/31, the correlations among the six sensor-based traits became much weaker. At this stage of growth, the crop canopy was closed; and there was no dominant effect of soil on the canopy trait measurement. GPF and NDVI indices tended to saturate, and became less sensitive to soybean biomass accumulation. Because of full canopy, Tc-Ta was an indicator of the evaporative status of the canopy rather than fraction of vegetation. Due to these reasons, the strong correlations in the early season were not observed among these variables. Three NDVI indices were still significantly correlated with each other, but with lower correlation coefficient compared to the early season.

The inter-correlation among the sensor-based traits became stronger again on Sep/2. At this late stage, some plots entered into maturity with wilted leaves. These were also the plots that tended to have higher Tc-Ta (less evaporation), lower NDVI, and lower GPF (wilted leaves were not classified as green pixels). This was the main reason for a strong negative correlation between Tc-Ta and all other variables.

One big advantage of sensor-based traits is that repeated measurements can be taken throughout a season, which provides the opportunity to elucidate their temporal dynamics and plant growth pattern. Fig. 10 shows the six sensor-based traits (averaged over all 120 soybean plots) plotted with date. It can be seen that crop height increased steadily from Jun/30 to Aug/10. Height increase appeared to be faster in the early season (Jun/30 to Jul/21) than the mid-season (Jul/21 to Aug/10). Height on Sep/2 was lower than Aug/10, which was partly due to lodging of the soybean plants as they matured.

The two NDVI indices (NDVI-SRS and NDVI-spec) exhibited the same pattern, all rising sharply at the early season and approaching a plateau on Jul/21. Their consistency with each other again provided a validation of the performance of the NDVI sensors and the portable spectrometers. RE-NDVI-spec followed the same pat-

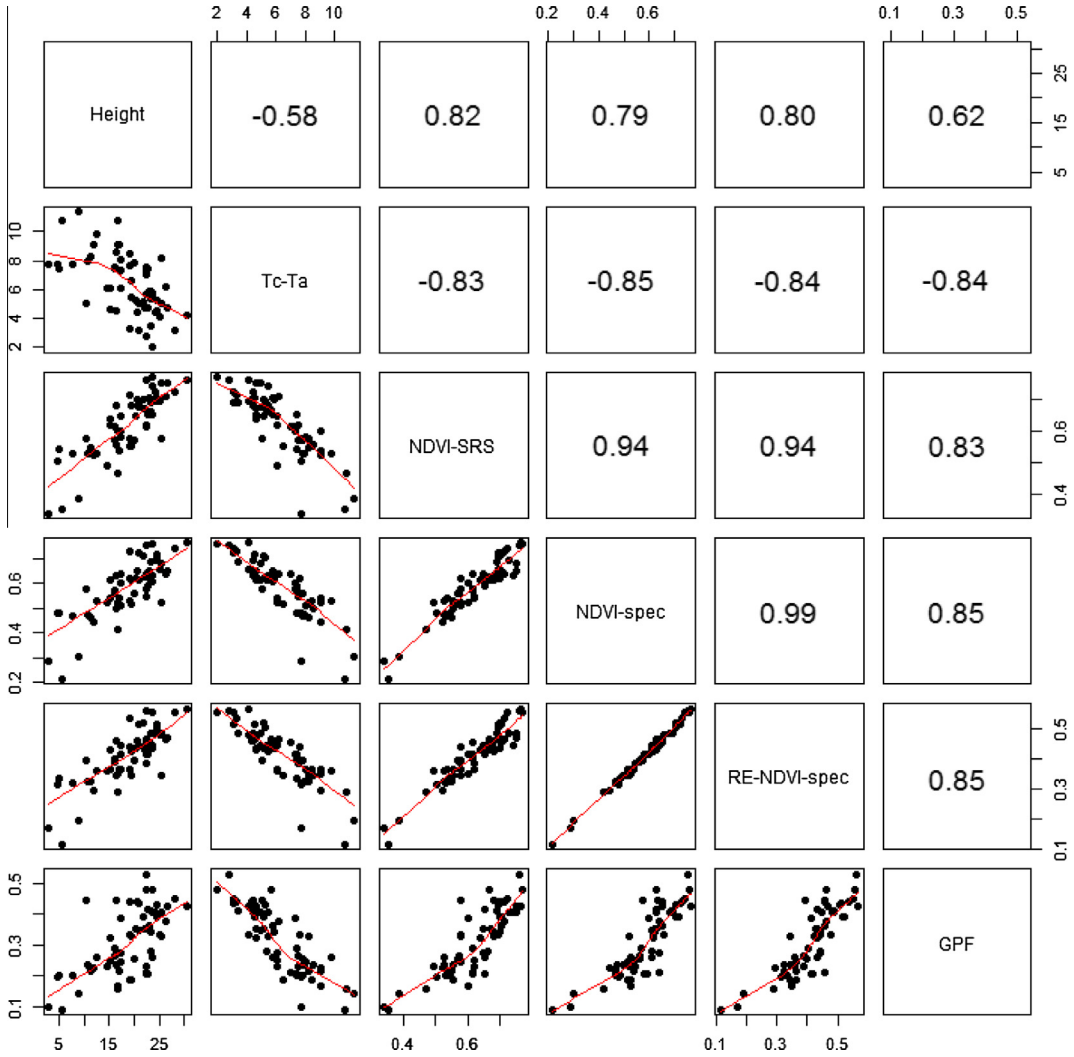

Fig. 7. The correlation matrix of the six soybean traits measured by the multi-sensor system at the plot level on Jun/30/2015. The upper triangle of the matrix denotes Pearson's correlation coefficients among the variables.

tern as NDVI, but had a lower amplitude and still showed sensitivity to biomass accumulation when NDVI indices were near saturation (Jul/21 to Aug/10). This is in agreement with the literature that proposes to use red-edge NDVI as a more responsive index when vegetation canopy is full. All three spectral indices showed decrease on Sep/2. This was due to maturation and some sign of late season drought that turned part of the canopy brown and yellow.

There was a continuous decrease in Tc-Ta from Jun/30 to Jul/30. This was due to the accumulation of biomass during which the soil fraction became smaller and smaller in TIR sensor's field of view. At late season, Tc is about 1.5 °C below Ta. This was to be expected because evaporative cooling made the canopy temperature lower that air temperature.

GPF indicated a fast plant growth from Jun/30 to Jul/8. But the index stayed almost constant from Jul/8 to Aug/10. Fig. 6 shows that plots reached full canopy coverage between Jul/8 and Jul/21, making it not responsive to plant growth (whereas the height, Tc-Ta, and NDVI were still responsive). At these dates, average GPF was between 0.53 and 0.58 (approximately half of the pixels were classified as background). Since we know canopy was full, this apparent bias was caused by the fraction of canopy that was shaded (dark pixels) and misclassified as background (see Fig. 6). On 9/2 average GFP dropped significantly to 0.44. This was because the canopy turned yellow as soybean matured.

3.4. Correlation between sensor-based measurements and yield

Yield is commonly the most important trait and the main focus of breeding programs. Therefore, a critical question posed by breeders for high throughput field phenotyping systems is that whether the traits captured by sensors can be related to the final yield. If a sensor-based trait measured at a particular growth stage is found to be consistently highly correlated with yield, it indicates this trait can potentially be used to assist the selection process; or to recover data from trials lost to adverse conditions after the sensor-based trait was measured (e.g., late season hail). Table 2 gives Pearson's correlation between the six in-season, sensor-based traits and final grain yield of soybean.

When comparing among the sensor-based traits, it appears that all of them have comparable predictive power to soybean yield, with GPF showing a slightly higher overall correlation followed by NDVI indices and then Tc-Ta and Height.

The correlations with grain yield tend to be higher at both early (Jun/30) season and late (Sep/2) season, but low in the mid-season. While the same correlation structures are observed at these two

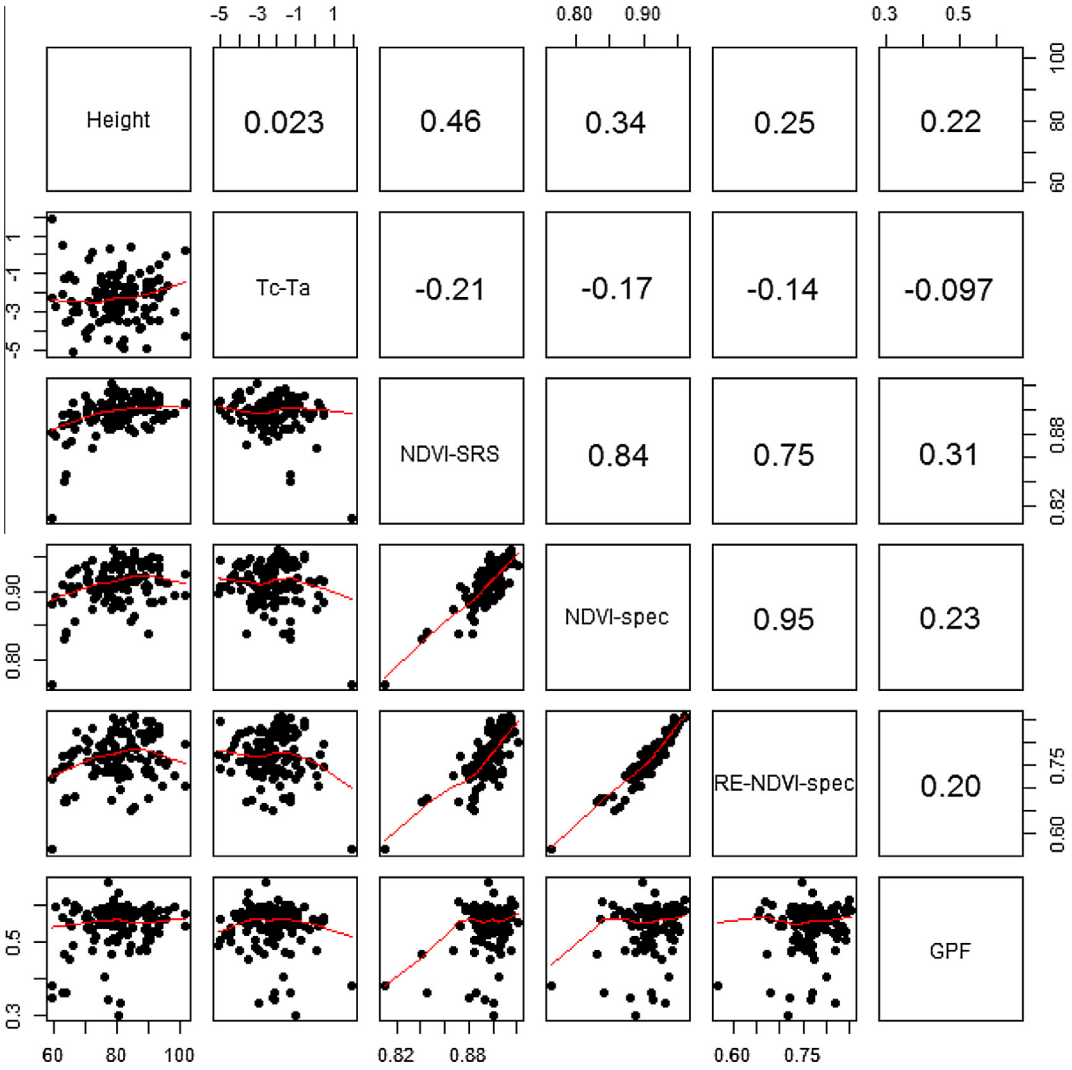

Fig. 8. The correlation matrix of the six soybean traits measured by the multi-sensor system at the plot level on Jul/31/2015. The upper triangle of the matrix denotes Pearson's correlation coefficients among the variables.

stages, we reason that they were determined by different underlying mechanisms. The strong correlations at early season were driven by vegetation coverage, which indicated that establishing larger vegetative stature and accumulating high biomass can be beneficial for yield. This result is encouraging because these sensor-based traits can be applied at very early season to guide selection and potentially accelerate the pace of breeding.

At the late reason (Sep/2), the strong correlations seemed to be driven by wilted versus still healthy canopy in the plots. Healthy canopy at this stage indicated a prolonged grain filling which often increased the final yield. What captured by the various sensor modules were essentially similar to the "stay green" trait commonly used by the breeders for late reason growth and resource utilization.

3.5. Future development and testing of the sensor system for high throughput field phenotyping

In the short term, we will expand the capability in system's software to process reflectance spectra and RGB images in real time fashion. This would eliminate tedious post processing, improve the throughput of data analysis, and allow breeders to assess phenotype data immediately after data collection. In addition to NDVI and RE-NDVI, other spectral indices such as PRI and SIF can be extracted from the reflectance spectra. These additional spectral indices can be proxies for different aspects of plant physiological response to environmental stresses. Processing RGB images in real time requires more demanding computing power of the host computer, which can be a practical challenge for real time computing.

In the long term, we will explore to integrate more advanced sensor modules into this multi-sensor system. Low-cost depth imaging sensors (for example, Microsoft Kinect), LIDAR (Light Detection and Ranging), light curtain, and multi/hyper spectral imaging are deemed promising technologies for plant phenotyping, and they are now extensively tested in the controlled environments (Fanourakis et al., 2014; Ge et al., 2016; Paulus et al., 2014a, 2014b). Adoption of these sensor modules in the field for an integrated plant phenotyping system is challenging for the following reasons. First, they are susceptible to environment variations such as sun illumination, temperature, humidity, wind and mechanical vibration. Second, they usually require dedicated controlling unit and specialized software to operate, making it not easy for system level integration. In terms of LIDAR and hyperspectral imaging, the volume of data generated is huge, and data post processing for information extraction is almost inevitable. Therefore, to seam-

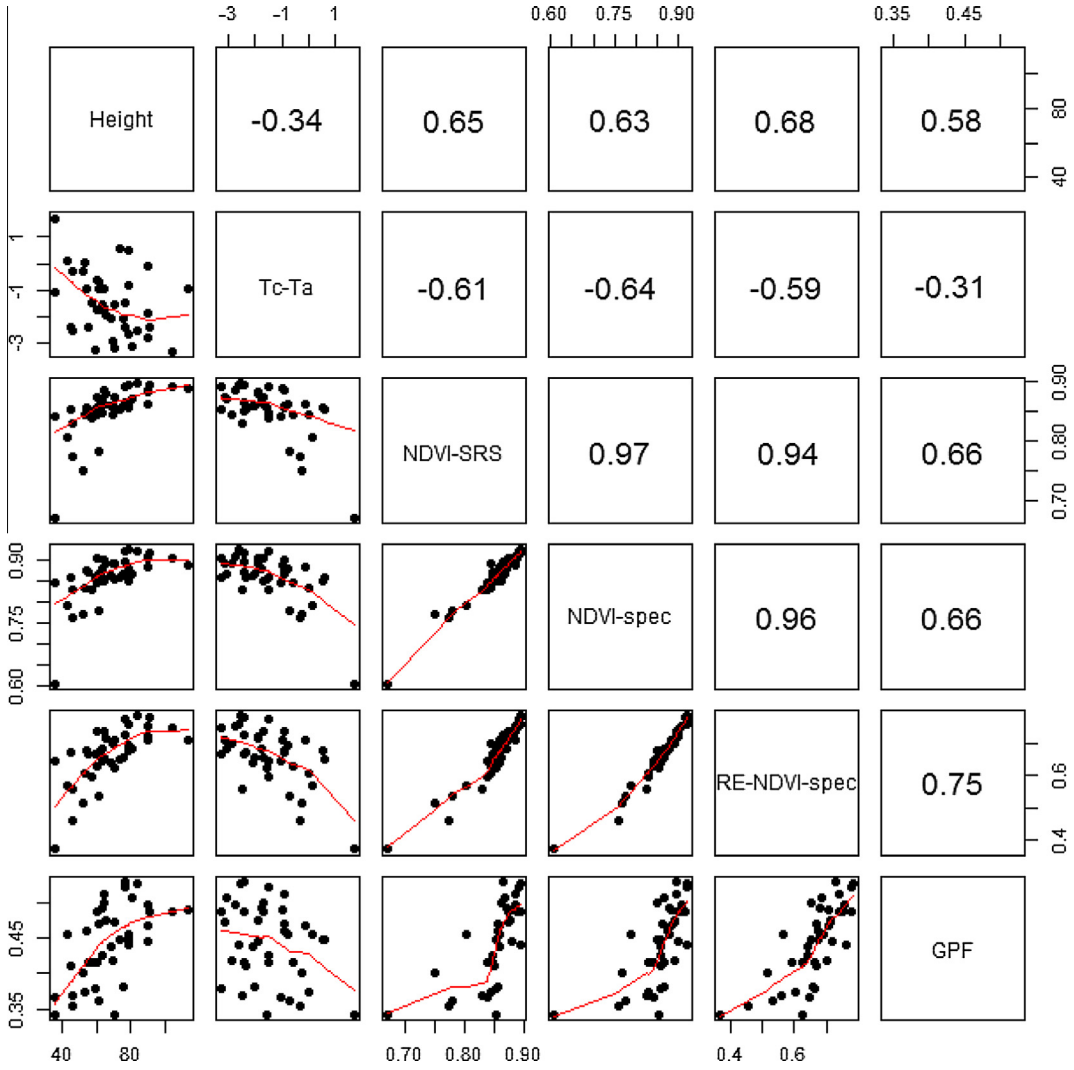

Fig. 9. The correlation matrix of six soybean traits measured by the multi-sensor system at the plot level on Sep/02/2015. The upper triangle of the matrix denotes Pearson's correlation coefficients among the variables.

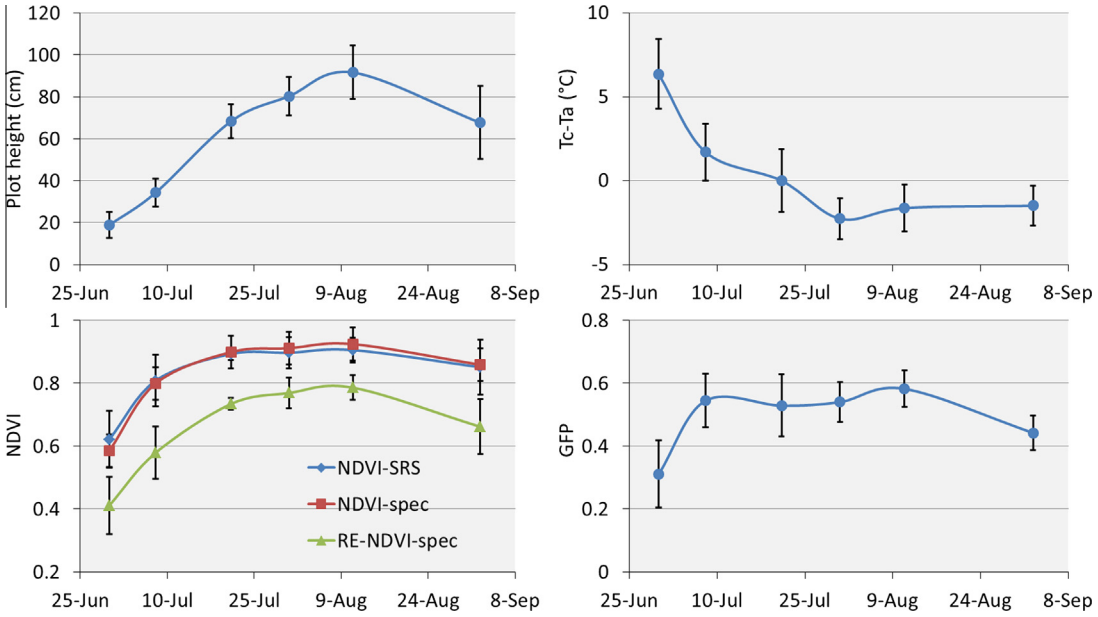

Fig. 10. The six sensor-based plot traits measured by the sensor system at different dates. The values are the average over all 120 soybean plots; and the standard deviations are indicated as error bars.

Table 2
Pearson's correlations between sensor-based trait measurements and final grain yield of soybean.

Experiment date	Height	Tc-Ta	NDVI-SRS	NDVI-spec	RE-NDVI-spec	GPF
June 30	0.41**	−0.51***	0.50***	0.49***	0.46**	0.55***
July 8	0.22 ns	−0.03 ns	0.29*	0.27*	0.25 ns	−0.38**
July 21	0.20*	−0.35***	0.34***	0.19*	0.05 ns	0.36***
July 31	0.37***	−0.14 ns	0.48***	0.40***	0.28**	0.10 ns
August 11	0.54***	−0.48***	0.57***	0.51***	0.41***	0.20*
September 2	0.60***	−0.55***	0.65***	0.65***	0.68***	0.70***

ns – Not significant.
*** Significant at 0.001 level.
** Significant at 0.01 level.
* Significant at 0.05 level.

lessly bring these advanced sensors into the current multi-sensor system is not trivial; and such efforts may rely on future advancements of the sensor modules, computing power, and data analytics.

4. Conclusion

In this paper, we reported an integrated sensor system aiming at high throughput field phenotypic data collection for plant breeding. The system comprised five sensing modules: ultrasonic distance sensors, infrared thermal radiometers, NDVI sensors, portable spectrometers and RGB cameras. In addition, the system also integrated a solar radiation sensor and air temperature/relative humidity sensor to measure environmental variables. From these sensors six crop canopy traits were extracted: height, temperature, two NDVI indices, red-edge NDVI index, and green pixel fraction. A LabVIEW program was developed to control and synchronize sensor measurements and store them on the computer for further analysis. The sensor system was tested in a soybean and wheat field with satisfactory and robust performance. Results of data analysis showed strong inter-correlations among the sensor-based traits, providing an internal validation of the reliability of sensors in field data collection. Plotting the sensor-based traits as a function of time (as allowed by repeated field measurements during the season) provided the characterization of the temporal dynamics of these traits. Strong correlations were also found between all six sensor based traits and final grain yield of soybean, suggesting the usefulness of the sensor system in plant breeding.

Acknowledgements

The funding for this work is provided by National Science Foundation of the United States (DBI-1556186), Nebraska Soybean Board, Nebraska Wheat Board, and Agricultural Research Division of University of Nebraska-Lincoln.

Appendix A. Supplementary material

Supplementary data associated with this article can be found, in the online version, at http://dx.doi.org/10.1016/j.compag.2016.08.021.

References

Andrade-Sanchez, P., Gore, M.A., Heun, J.T., Thorp, K.R., Carmo-Silva, A.E., French, A. N., Salvucci, M.E., White, J.W., 2014. Development and evaluation of a field-based high-throughput phenotyping platform. Funct. Plant Biol. 41, 68–79.
Ahamed, T., Tian, L., Jiang, Y., Zhao, B., Liu, H., Ting, K.C., 2012. Tower remote-sensing system for monitoring energy crops; image acquisition and geometric corrections. Biosyst. Eng. 112, 93–107.
Araus, J.L., Cairns, J.E., 2013. Field high-throughput phenotyping: the new crop breeding frontier. Trends Plants Sci. 19, 52–61.
Campbell, M.T., Knecht, A.C., Berger, B., Brien, C.J., Wang, D., Walia, H., 2015. Integrating image-based phenomics and association analysis to dissect the genetic architecture of temporal salinity responses in rice. Plant Physiol. 168, 1476–1489.
Comar, A., Burger, P., de Solan, B., Baret, F., Daumard, F., Hanocq, J.-F., 2012. A semi-automatic system for high throughput phenotyping wheat cultivars in-field conditions: description and first results. Funct. Plant Biol. 39, 914–924.
Deery, D., Jimenez-Berni, J., Jones, H., Sirault, X., Furbank, R., 2014. Proximal remote sensing buggies and potential applications for field-based phenotyping. Agronomy 5, 349–379.
Fahlgren, N., Feldman, M., Gehan, M., Wilson, M.S., Shyu, C., Bryant, D.W., Hill, S.T., McEntee, C.J., Warnasooriya, S.N., Kumar, I., Ficor, T., Turnipseed, S., Gilbert, K.B., Brutnell, T.P., Carrington, J.C., Mockler, T.C., Baxter, I., 2015. A versatile phenotyping system and analytics platform reveals diverse temporal responses to water availability in Setaria. Molecul. Plant 8, 1–16.
Fanourakis, D., Briese, C., Max, J.F.J., Kleinen, S., Putz, A., Fiorani, F., Ulbrich, A., Schurr, U., 2014. Rapid determination of leaf area and plant height by using light curtain arrays in four species with contrasting shoot architecture. Plant Meth. 10, 9.
Farooque, A.A., Chang, Y.K., Zaman, Q.U., Groulx, D., Schumann, A.W., Esau, T.J., 2013. Performance evaluation of multiple ground based sensors mounted on a commercial wild blueberry harvester to sense plant height, fruit yield and topographic features in real-time. Comput. Electron. Agri. 91, 135–144.
Furbank, R.T., Tester, M., 2011. Phenomics – technologies to relieve the phenotyping bottleneck. Trends Plant Sci. 16 (12), 635–644.
Gamon, J.A., Serrano, L., Surfus, J.S., 1997. The photochemical reflectance index: an optical indicator of photosynthetic radiation use efficiency across species, functional types, and nutrient levels. Oecologia 112, 492–501.
Garbulsky, M.F., Peñuelas, J., Gamon, J., Inoue, Y., Filella, I., 2011. The photochemical reflectance index (PRI) and the remote sensing of leaf, canopy and ecosystem radiation use efficiencies: a review and meta-analysis. Remote Sens. Environ. 115, 281–297.
Ge, Y., Bai, G., Stoerger, V., Schnable, J.C., 2016. Temporal dynamics of maize plant growth, water use, and leaf water content using automated high throughput RGB and hyperspectral imaging. Comput. Electron. Agri. 127, 625–632.
Guanter, L., Rossini, M., Colombo, R., Meroni, M., Frankenberg, C., Lee, J.-E., Joiner, J., 2013. Using field spectroscopy to assess the potential of statistical approaches for the retrieval of sun-induced chlorophyll fluorescence from ground and space. Remote Sens. Environ. 133, 52–61.
Kipp, S., Mistele, B., Baresel, P., Schmidhalter, U., 2014. High-throughput phenotyping early plant vigor of winter wheat. Eur. J. Agron. 52, 271–278.
Meroni, M., Rossini, M., Guanter, L., Alonso, L., Rascher, U., Colombo, R., Moreno, J., 2009. Remote sensing of solar-induced chlorophyll fluorescence: review of methods and applications. Remote Sens. Environ. 113, 2037–2051.
Montes, J.M., Technow, F., Dhillon, B.S., Mauch, F., Melchinger, A.E., 2011. High-throughput non-destructive biomass determination during early plant development in maize under field conditions. Field Crops Res. 121, 268–273.
Nelissen, H., Moloney, M., Inzé, D., 2014. Translational research: from pot to plot. Plant Biotechnol. J. 12, 277–285.
Noh, H., Zhang, Q., Shin, B., Han, S., Feng, L., 2006. A neural network model of maize crop nitrogen stress assessment for a multi-spectral imaging sensor. Biosyst. Eng. 94, 477–485.
Passioura, J.B., 2012. Phenotyping for drought tolerance in grain crops: when is it useful to breeders? Funct. Plant Biol. 39, 851–859.
Paulus, S., Behmann, J., Mahlein, A.K., Plumer, L., Kuhlmann, H., 2014a. Low-cost 3D systems: suitable tools for plant phenotyping. Sensors 14, 3001–3018.
Paulus, S., Schumann, H., Kuhlmann, H., Léon, J., 2014b. High-precision laser scanning system for capturing 3D plant architecture and analysis growth of cereal plants. Biosyst. Eng. 121, 1–11.
Ray, D.K., Ramankutty, N., Mueller, N.D., West, P.C., Foley, J.A., 2012. Recent patterns of crop yield growth and stagnation. Nat. Commun. 3, 1293.
Romano, G., Zia, S., Spreer, W., Sanchez, C., Cairns, J., Araus, J.L., Müller, J., 2011. Use of thermography for high throughput phenotyping of tropical maize adaptation in water stress. Comput. Electron. Agri. 79, 67–74.
Sankaran, S., Khot, L.R., Espinoza, C.Z., Jarolmasjed, S., Santhuvalli, V.R., Vandemark, G.J., Miklas, P.N., Carter, A.H., Pumphrey, M.O., Knowles, N.R., Pavek, M.J., 2015.

Low-altitude, high-resolution aerial imaging systems for row and field crop phenotyping: a review. Eur. J. Agron. 70, 112–123.
Scotford, I.M., Miller, P.C.H., 2004. Estimating tiller density and leaf area index of winter wheat using spectral reflectance and ultrasonic sensing techniques. Biosyst. Eng. 89, 395–408.
Sharma, B., Ritchie, G.L., 2015. High-throughput phenotyping of cotton in multiple irrigation environments. Crop Sci. 55, 958–969.
Shendure, J., Ji, H., 2008. Next-generation DNA sequencing. Nat. Biotechnol. 26, 1135–1145.
Sims, D.A., Gamon, J.A., 2002. Relationships between leaf pigment content and spectral reflectance across a wide range of species, leaf structures and developmental stages. Remote Sens. Environ. 81, 337–354.
Sui, R., Thomasson, J.A., Hanks, J., Wooten, J., 2008. Ground-based sensing system for weed mapping in cotton. Comput. Electron. Agri. 60, 31–38.
Sui, R., Thomasson, J.A., 2006. Ground-based sensing system for cotton nitrogen status determination. Trans. ASABE 49, 1983–1991.
Wang, P., Lan, Y., Luo, X., Zhou, Z., Wang, Z., Wang, Y., 2014. Integrated sensor system for monitoring rice growth conditions based on unmanned ground vehicle. Int. J. Agri. Biol. Eng. 7, 75–81.
White, J.W., Conley, M.M., 2013. A flexible, low-cost cart for proximal sensing. Crop Sci. 53, 1646–1649.
White, J.W., Andrade-Sanchez, P., Gore, M.A., Bronson, K.F., Coffelt, T.A., et al., 2012. Field-based phenomics for plant genetics research. Field Crops Res. 133, 101–122.
Winterhalter, L., Mistele, B., Jampatong, S., Schmidhalter, U., 2011. High throughput phenotyping of canopy water mass and canopy temperature in well-watered and drought stressed tropical maize hybrids in the vegetative stage. Eur. J. Agron. 35, 22–32.